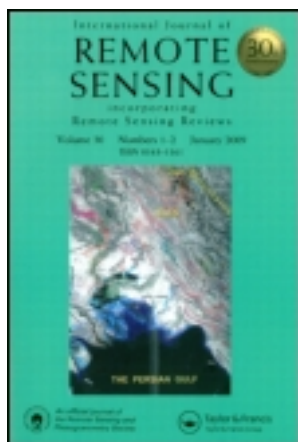


This article was downloaded by: [University of Oklahoma Libraries]

On: 14 October 2013, At: 23:23

Publisher: Taylor & Francis

Informa Ltd Registered in England and Wales Registered Number: 1072954 Registered office: Mortimer House, 37-41 Mortimer Street, London W1T 3JH, UK



International Journal of Remote Sensing

Publication details, including instructions for authors and subscription information:

<http://www.tandfonline.com/loi/tres20>

Comparison of PERSIANN and V7 TRMM Multi-satellite Precipitation Analysis (TMPA) products with rain gauge data over Iran

Saber Moazami^{ab}, Saeed Golian^c, M. Reza Kavianpour^a & Yang Hong^{bd}

^a School of Civil Engineering, K.N. Toosi University of Technology, Tehran, Iran

^b Advanced Radar Research Centre, University of Oklahoma, Norman, OK, USA

^c Civil Engineering Department, Shahrood University of Technology, Shahrood, Iran

^d School of Civil Engineering and Environmental Sciences, University of Oklahoma, Norman, OK, USA

Published online: 23 Sep 2013.

To cite this article: Saber Moazami, Saeed Golian, M. Reza Kavianpour & Yang Hong (2013) Comparison of PERSIANN and V7 TRMM Multi-satellite Precipitation Analysis (TMPA) products with rain gauge data over Iran, *International Journal of Remote Sensing*, 34:22, 8156-8171, DOI: [10.1080/01431161.2013.833360](https://doi.org/10.1080/01431161.2013.833360)

To link to this article: <http://dx.doi.org/10.1080/01431161.2013.833360>

PLEASE SCROLL DOWN FOR ARTICLE

Taylor & Francis makes every effort to ensure the accuracy of all the information (the "Content") contained in the publications on our platform. However, Taylor & Francis, our agents, and our licensors make no representations or warranties whatsoever as to the accuracy, completeness, or suitability for any purpose of the Content. Any opinions and views expressed in this publication are the opinions and views of the authors, and are not the views of or endorsed by Taylor & Francis. The accuracy of the Content should not be relied upon and should be independently verified with primary sources of information. Taylor and Francis shall not be liable for any losses, actions, claims, proceedings, demands, costs, expenses, damages, and other liabilities whatsoever or

howsoever caused arising directly or indirectly in connection with, in relation to or arising out of the use of the Content.

This article may be used for research, teaching, and private study purposes. Any substantial or systematic reproduction, redistribution, reselling, loan, sub-licensing, systematic supply, or distribution in any form to anyone is expressly forbidden. Terms & Conditions of access and use can be found at <http://www.tandfonline.com/page/terms-and-conditions>

Comparison of PERSIANN and V7 TRMM Multi-satellite Precipitation Analysis (TMPA) products with rain gauge data over Iran

Saber Moazami^{a,b*}, Saeed Golian^c, M. Reza Kavianpour^a, and Yang Hong^{b,d}

^aSchool of Civil Engineering, K.N. Toosi University of Technology, Tehran, Iran; ^bAdvanced Radar Research Centre, University of Oklahoma, Norman, OK, USA; ^cCivil Engineering Department, Shahrood University of Technology, Shahrood, Iran; ^dSchool of Civil Engineering and Environmental Sciences, University of Oklahoma, Norman, OK, USA

(Received 28 February 2013; accepted 14 July 2013)

The objective of this research is to evaluate daily rain rates derived from three widely used high-resolution satellite precipitation products (PERSIANN, TMPA-3B42V7, and TMPA-3B42RT) using rain gauge observations over the entire country of Iran. Evaluations are implemented for 47 comprehensive daily rainfall events during the winter and spring seasons from 2003 to 2006. These events are selected because each encompasses more than 50% of the country's area. In this study, daily rainfall observations derived from 1180 rain gauges distributed throughout the country are employed as reference surface data. Six statistical indices: bias, multiplicative bias (MBias), relative bias (RBias), mean absolute error (MAE), root mean square error (RMSE), and linear correlation coefficient (CC), as well as a contingency table are applied to evaluate the satellite rainfall estimates qualitatively. The spatially averaged results over the entire country indicate that 3B42V7, with an average bias value of -1.47 mmd^{-1} , RBias of -13.6% , MAE of 4.5 mmd^{-1} , RMSE of 6.5 mmd^{-1} , and CC of 0.61, leads to better estimates of daily precipitation than those of PERSIANN and 3B42RT. Furthermore, PERSIANN with an average MBias value of 0.56 tends to underestimate precipitation, while 3B42V7 and 3B42RT with average MBias values of 0.86 and 1.02, respectively, demonstrate a reasonable agreement in regard to rainfall estimations with the rain gauge data. With respect to the categorical verification technique implemented in this study, PERSIANN exhibits better results associated with the probability of detection of rainfall events; however, its false alarm ratio is worse than that of 3B42V7 and 3B42RT.

1. Introduction

Lack of a reliable and extensive observing system is one of the most important challenges in rainfall analysis, hydrologic predictions, and water resources management in Iran. In fact, the availability of high-quality ground rainfall data is very limited across many parts of this country. As an alternative source, satellite precipitation products, which provide high spatial coverage of input data for various hydrologic models, can be useful for data-sparse and ungauged basins in developing countries like Iran.

The use of satellite rainfall estimate (SRE) algorithms has been of growing interest for rainfall measurement over the past two decades. A number of new global high-resolution

*Corresponding author. Email: saber.moazami@ou.edu

SREs are now available, including the Precipitation Estimation from Remotely Sensed Information using Artificial Neural Networks (PERSIANN; Hsu et al. 1997; Sorooshian et al. 2000), the PERSIANN Cloud Classification System estimation (PERSIANN-CCS; Hong et al. 2004), the National Oceanic and Atmospheric Administration (NOAA) Climate Prediction Center (CPC) Morphing technique product (CMORPH; Joyce et al. 2004), the Naval Research Laboratory Global Blended Statistical Precipitation Analysis data (NRL-Blend; Turk and Miller 2005), the Tropical Rainfall Measuring Mission (TRMM) Multi-satellite Precipitation Analysis (TMPA; Huffman et al. 2007), and the Global Satellite Mapping of Precipitation (GSMaP; Kubota et al. 2009; Ushio et al. 2009). These satellite precipitation products have provided high temporal (≤ 3 h) and spatial ($\leq 0.25^\circ$) resolution precipitation maps.

Nevertheless, satellite precipitation products, due to their indirect nature of estimates, need be evaluated against *in situ* observations before application to daily and sub-daily hydrological operations (Jiang et al. 2012). Evaluation of SREs has been carried out for different spatial and temporal resolutions (Hong et al. 2006; Tian et al. 2007; Su, Hong, and Lettenmaier 2008; Li et al. 2009; Dinku, Connor, and Ceccato 2010; Hirpa, Gebremichael, and Hopson 2010; Behrangi et al. 2011; Bitew and Gebremichael 2011; AghaKouchak et al. 2012; Yong et al. 2012). There have also been attempts to assess the performance of satellite precipitation products over various regions with different physiographic and climate conditions. Hughes (2006) compared satellite rainfall data from PERSIANN and the Global Precipitation Climatology Project (GPCP) with observations from gauging station networks in four basins with different climate regimes within southern Africa to explore the use of SRE in hydrological models. Xie et al. (2007) developed a new gauge analysis product over East Asia and validated it against five high-resolution SREs (CMORPH, TRMM 3B42, 3B42RT, Naval Research Laboratory (NRL), and PERSIANN). Hong et al. (2007) validated the space–time structure of remotely sensed precipitation estimates to improve their quality and confident application in water cycle-related research. In their study, the performance of the PERSIANN Cloud Classification System (CCS) product was evaluated against warm season precipitation observations from the North American Monsoon Experiment (NAME) Event Rain Gauge Network (NERN) in the complex terrain region of northwestern Mexico. Habib, Henschke, and Adler (2009) focused on the evaluation of 3 hourly $0.25^\circ \times 0.25^\circ$ TMPA data during six heavy rainfall events that had been generated by tropical storms passing over Louisiana, USA. Yong et al. (2010) studied two standards of TMPA products, 3B42RT and 3B42V6, that were quantitatively evaluated in the Laohahe basin, China. As-Syakur et al. (2010) compared daily, monthly, and seasonal rain rates derived from TMPA using rain gauge analysis in the Bali islands. Romilly and Gebremichael (2011) evaluated three SRE products (TMPA-3B42RT, PERSIANN, and CMORPH) against collocated rain gauge measurements in Ethiopia across six river basins representing different rainfall regimes and topography. These studies highlighted that different types of satellite precipitation data have variable accuracy in different regions. Therefore, for a certain region it is important to determine which product is the best (Jiang et al. 2012). It should be noted that for Iran, which is the subject of this research, only one study associated with verification of satellite-based rainfall products is available (Javanmard et al. 2010). It compared TRMM-3B42V6 rainfall estimates with gridded precipitation data sets ($0.25^\circ \times 0.25^\circ$ latitude/longitude) for the entire country of Iran. The results indicated that version 6 of TRMM-3B42 underestimates (by around 25%) mean annual precipitation over the entire country, with a value of 0.17 mm/day.

In this study, we compare daily rainfall estimations of three widely used high-resolution satellite precipitation products including PERSIANN, the TMPA adjusted product of

version 7 (3B42V7), and the TMPA real-time product (3B42RT) with rain gauge observations as a reference data set over Iran. The approach of evaluations presented here differs from that of Javanmard et al. (2010) in that it makes direct comparison of various satellite precipitation products with a dense rain gauge network (1180 rain gauges) distributed over 900 grid boxes of $0.25^\circ \times 0.25^\circ$ (corresponding to PERSIANN and TMPA pixel size) throughout the country. Also, Javanmard et al. (2010) employed an interpolation technique based on Yatagai, Xie, and Alpert (2008) to derive gridded data sets from 337 climatology stations distributed throughout the country. However, such a small number of rainfall stations would significantly influence the accuracy of interpolation. Note that in our study, in order to achieve more accurate verification, we did not use any interpolation technique to predict rain gauge values for those grid boxes lacking gauges. Hence, only 900 grid boxes are involved in the assessments, each containing at least one rain gauge.

The present work is organized as follows: Section 2 introduces the study area and data resources used; Section 3 describes the implemented methodology for evaluating the SREs; Section 4 details the results and discussions; and Section 5 presents the summary and conclusions.

2. Study area and data

2.1. Study area

The study area of this research is the country of Iran (25° – 40° N, 44° – 64° E) with a total area of 1,648,195 km². As shown in Figure 1(a), Iran is a mountainous country in which 60% is covered by two mountain ranges, the Alborz Mountains in the northern part and the Zagros Mountains in the western and southwestern parts of country. However, the central parts of the country are covered by two dry deserts, the Dasht-e-Kavir and Dasht-e-Lut. Therefore, a considerable part of the country has an arid or semiarid climate. However, the regions close to the Caspian Sea and some close to the Persian Gulf and Sea of Oman have humid weather, with large annual rainfall over the Caspian coast. These various conditions of terrain and topography play a significant role in climate regimes, so there are large temporal and spatial variations of precipitation over the country. The average annual rainfall for the entire country is about 250 mm, ranging from 50 mm in desert areas to 1600 mm for the Caspian Sea coastal area (Figure 1(b), Javanmard et al. 2010). Note that the topography of Iran is rugged, with elevation ranging from 300 to 5600 m (see Figure 1(a)).

2.2. Data sets

The reference data sets employed in the present work are based on the daily rainfall observations derived from 940 rain gauges and 240 synoptic stations. Rain gauge and synoptic station data were provided by the Iran Water Resources Management Co. (IWRM) and Iran Meteorological Organization (IMO), respectively. Notice that throughout this article, the expression ‘rain gauges’ is used for combined rain gauges and synoptic stations (i.e. 1180 gauges) over the study area to simplify the presentation.

The satellite rainfall products used in this study are based on PERSIANN, TMPA-3V42V7, and TMPA-3B42RT. The PERSIANN system uses neural network function classification/approximation procedures to compute an estimate of rainfall rate at each $0.25^\circ \times 0.25^\circ$ pixel of the infrared (IR) brightness temperature (T_b) image provided by geostationary satellites. An adaptive training feature facilitates updating of the network parameters whenever independent estimates of rainfall are available. The PERSIANN system is based on geostationary infrared imagery and was later extended to include the use

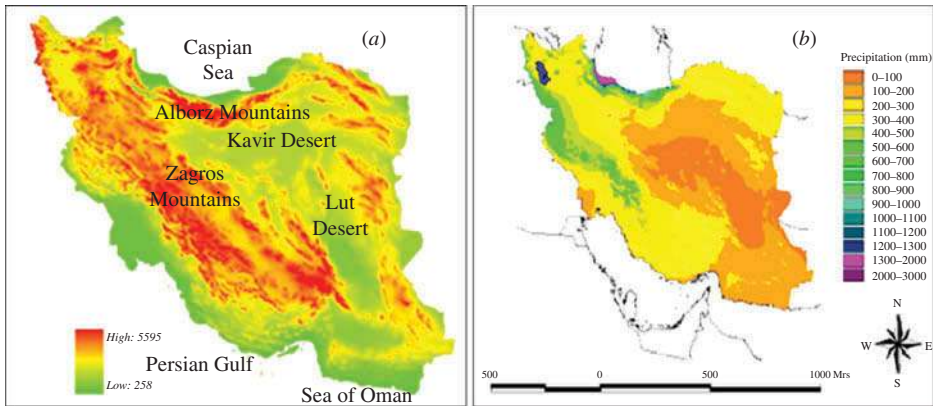


Figure 1. (a) Elevation map of Iran; (b) mean annual precipitation (mm) across Iran, 1961–1990 (Javanmard et al. 2010).

of both infrared and daytime visible imagery. The PERSIANN algorithm used here is based on the geostationary long-wave infrared imagery to generate global rainfall. Rainfall products are available from 50° S to 50° N globally. The system uses grid infrared images from global geosynchronous satellites (GOES-8, GOES-10, GMS-5, Metsat-6, and Metsat-7) provided by CPC, NOAA, to generate 30 min rain rates, which are aggregated to 6 hour accumulated rainfall. Model parameters are regularly updated using rainfall estimates from low-orbital satellites, including TRMM, NOAA -15, -16, -17, and DMSP (Defense Meteorological Satellite Program) F13, F14, and F15. In this study, the 6 hour temporal and $0.25^{\circ} \times 0.25^{\circ}$ latitude/longitude spatial scales of PERSIANN data were employed according to the website, <http://chrs.web.uci.edu/>. The daily PERSIANN data were then computed by aggregating 6 hour data into 24 hour data in order to synchronize satellite estimates with rain gauge measurements.

The NASA Goddard Earth Sciences Data and Information Services Center (GES DISC) announced the release of version 7 TRMM TMPA products with near-global (50° S– 50° N) coverage. The TMPA estimates are available in the form of two products, a near-real-time version (TMPA-RT) and a post-real-time research version. The sources of passive microwave satellite precipitation estimates include the TRMM Microwave Imager (TMI), Special Sensor Microwave Imager (SSM/I), Special Sensor Microwave Imager/Sounder (SSMIS), Advanced Microwave Scanning Radiometer-EOS (AMSR-E), Advanced Microwave Sounding Unit-B (AMSU-B), and Microwave Humidity Sounder (MHS) (more details can be found in Huffman et al. 2011; Huffman and Bolvin 2012).

There are four TMPA-RT products, namely the combined 3 hourly high-quality (HQ) and variable rain rate (VAR) product (3B42RT), HQ product (3B40RT), VAR product (3B41RT), and 3B42RT derived daily product. Also, the post-real-time data of version 7 consist of three products at different temporal resolutions: 3 hourly (3B42), daily (3B42-derived), and monthly (3B43). The spatial resolution for all abovementioned products is $0.25^{\circ} \times 0.25^{\circ}$.

The 3B42V7 incorporates the latest version 4 of Global Precipitation Climatology Centre (GPCC) full-gauge analysis from 1998 to 2010 and the GPCC monitoring gauge analysis since 2010. The 3B42V7 and 3B42RT at 3 hour temporal scale are used in this study and can be obtained from the TRMM website at <http://disc2.nascom.nasa.gov/tovas/>.

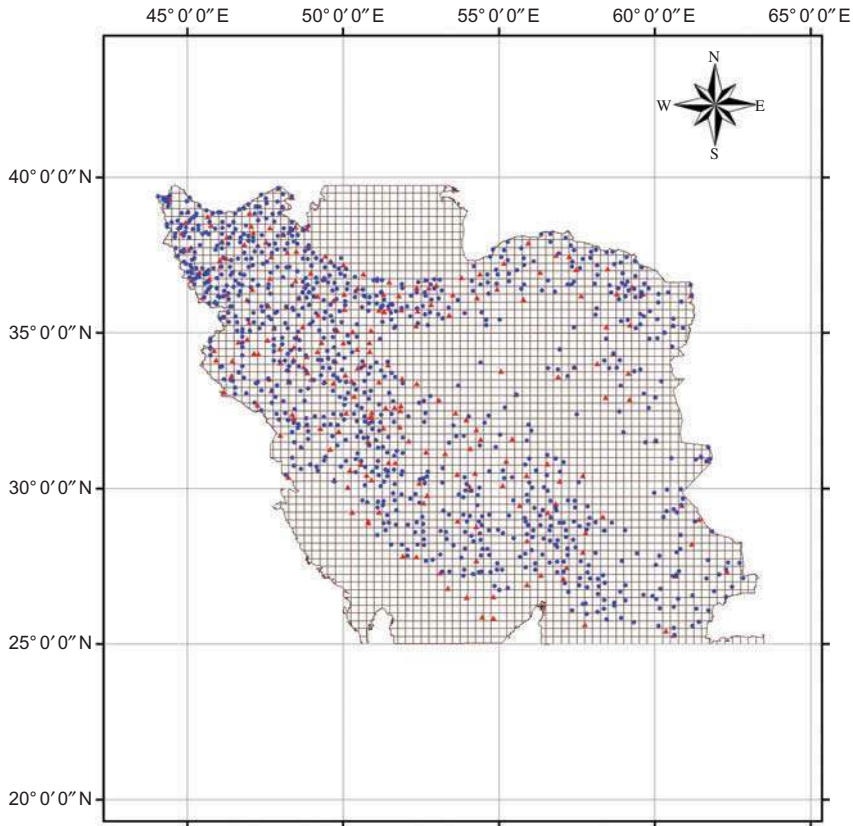


Figure 2. Map of rain gauges (circles), synoptic stations (triangles), and satellite data set grid boxes in Iran.

The daily data were then computed by aggregating 3 hour temporal resolution data over 24 hours for both TMPA products.

It should be pointed out that the daily temporal resolution of SREs is used in this article because the reference rain gauge data are based on daily measurements. Indeed, no appropriate set of sub-daily ground data exists for the study area. Figure 2 shows the grid boxes with a spatial resolution of $0.25^\circ \times 0.25^\circ$ latitude/longitude (corresponding to PERSIANN and TMPA pixel size) over Iran. It also shows the location of rain gauges and synoptic stations employed in this study.

3. Methodology

3.1. Validation

In this study the evaluation of SREs was conducted for 47 large-scale daily rainfall events from 2003 to 2006. The authors tried to select those events based on their extent over the study area. Therefore, all of the events under this criterion occurred in the winter and spring, which are generally the rainy seasons over Iran. Note that the satellite-retrieved precipitation was recorded by snapshots and represents an areal rain rate at each pixel, while the rain gauge observation was continuous at a particular point. Therefore, comparison

between these two sources was implemented for 900 grid boxes each containing at least one rain gauge. The true areal average rainfall over a grid box is assumed to be the rainfall value measured by the rain gauge located within that grid box. Also, for a grid box with two or more rain gauges, the true areal average rainfall is the average value of those rain gauges located within it.

3.2. Evaluation statistics

To evaluate the performance of SREs, six continuous statistics were used in the present study. The bias is defined as the average difference between rain gauge observations and SREs, and can be either positive or negative. A negative bias indicates underestimation of rainfall while a positive bias indicates overestimation. The multiplicative bias (MBias) is the ratio of SREs to rain gauge value – a perfect value of estimation would result in an MBias of 1. Underestimation will lead to values less than 1, and overestimating to values greater than 1. The relative bias (RBias) describes the systematic bias of satellite-based precipitation and behaves the same as bias. The mean absolute error (MAE) is used to represent the average magnitude of the error. The root mean square error (RMSE), which gives a greater weight to the larger errors relative to MAE, is used to measure the average error magnitude. The correlation coefficient (CC) is used to assess the agreement between satellite-based precipitation and rain gauge observations. The value of CC is such that $-1 < CC < +1$. A CC value of exactly +1 indicates a perfect positive fit, while value of exactly -1 indicates a perfect negative fit. If there is no linear correlation or a weak linear correlation, CC is close to 0:

$$\text{Bias} = \frac{\sum_{i=1}^N (P_{S_i} - P_{O_i})}{N}, \quad (1)$$

$$\text{MBias} = \frac{\sum_{i=1}^N P_{S_i}}{\sum_{i=1}^N P_{O_i}}, \quad (2)$$

$$\text{RBias} = \frac{\sum_{i=1}^N (P_{S_i} - P_{O_i})}{\sum_{i=1}^N P_{O_i}} \times 100\%, \quad (3)$$

$$\text{MAE} = \frac{\sum_{i=1}^N |P_{S_i} - P_{O_i}|}{N}, \quad (4)$$

$$\text{RMSE} = \left[\frac{\sum_{i=1}^N (P_{S_i} - P_{O_i})^2}{N} \right]^{1/2}, \quad (5)$$

$$\text{CC} = \frac{\sum_{i=1}^N (P_{S_i} - \bar{P}_S) (P_{O_i} - \bar{P}_O)}{\sqrt{\sum_{i=1}^N (P_{S_i} - \bar{P}_S)^2} \sqrt{\sum_{i=1}^N (P_{O_i} - \bar{P}_O)^2}}, \quad (6)$$

where P_{S_i} is the value of SRE for the i th daily event, P_{O_i} is the value of rain gauge observation for the i th daily event, N is the number of daily rainfall events, \bar{P}_S is the average value of SREs for N daily events over each grid box, and \bar{P}_O is the average value of rain gauge observations for N daily events over each grid box.

In addition, three categorical statistical indices (Wilks 2006), including the probability of detection (POD), false alarm ratio (FAR), and critical success index (CSI), are used to assess the rain-detection capabilities of SREs. POD represents the ratio of the correct identification of rainfall by satellite product to the number of rainfall occurrences observed by reference data; FAR denotes the proportion of cases in which the satellite records rainfall when the rain gauges do not; and CSI shows the overall proportion of rainfall events correctly diagnosed by the satellite. POD, FAR, and CSI range from 0 to 1, with 1 being a perfect POD and CSI and 0 being a perfect FAR. These metrics are calculated based on Equations (7)–(9):

$$\text{POD} = \frac{N_H}{N_H + N_M}, \quad (7)$$

$$\text{FAR} = \frac{N_F}{N_H + N_F}, \quad (8)$$

$$\text{CSI} = \frac{N_H}{N_H + N_M + N_F}, \quad (9)$$

where N_H represents the number of times that observed rain is correctly detected, N_M is the number of times that observed rain is not detected, and N_F is the number of times that rain is detected but not observed. It will be noted in this study that a threshold of 1.0 mmd^{-1} is used to distinguish between rain and no rain.

4. Results and discussion

In this study for the first time, a comparison between daily rainfall values estimated by three widely used satellite products and rain gauge observations was implemented over the entire country of Iran. The evaluation of SREs is based on the 47 rainy days, each occurring over more than 50% of the country's area.

Figure 3 represents the average value of each selected daily rainfall event measured by rain gauges and the three satellite products over the grid boxes for that event. As will be seen in this figure, in the range $9\text{--}21 \text{ mmd}^{-1}$ for rain gauge values, PERSIANN indicates underestimation and 3B42RT overestimation. In this range, 3B42V7 expresses reasonable agreement with the rain gauge observations. Figure 4 shows the scatterplots of averaged daily rainfall over each selected grid box for the three satellite products versus the corresponding values from rain gauges. Also, the country-averaged values of statistical indices are shown in this figure. According to Figure 4(a), PERSIANN shows underestimation, particularly for rain rates higher than 10 mmd^{-1} . Moreover, in this figure, the values of MBias (0.56), bias (-4.8 mmd^{-1}), and RBias (-44.3%) confirm that PERSIANN seriously underestimated rainfall levels over the study area. In Figures 4(b) and (c), 3B42V7 with country-averaged values of 0.86, -1.47 mmd^{-1} , and -13.6% for MBias, bias, and RBias, respectively, shows underestimation, while 3B42RT with values of 1.02, 0.26 mmd^{-1} , and 2.38%, respectively, shows overestimation. Also according to Figure 4, 3B42 obtained the best values for MAE (4.5 mm), RMSE (6.5 mm), CC (0.61), FAR (0.44), and CSI (0.43), whereas PERSIANN obtained the best value for POD (0.93).

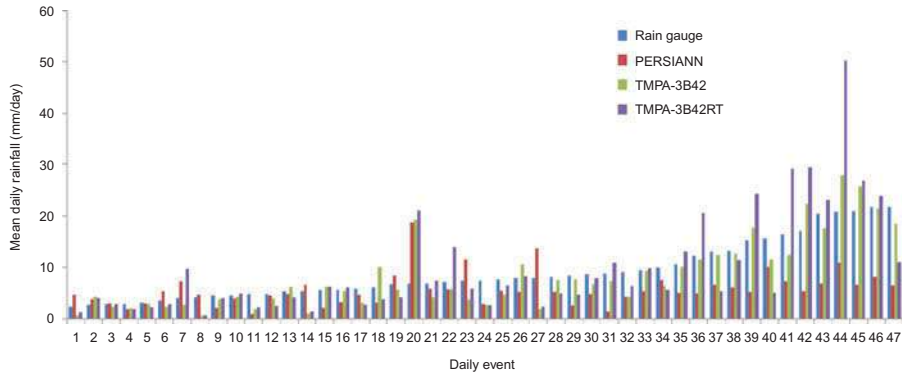


Figure 3. Average value of each selected daily rainfall event as measured by rain gauges and three satellite products over the grid boxes for that event.

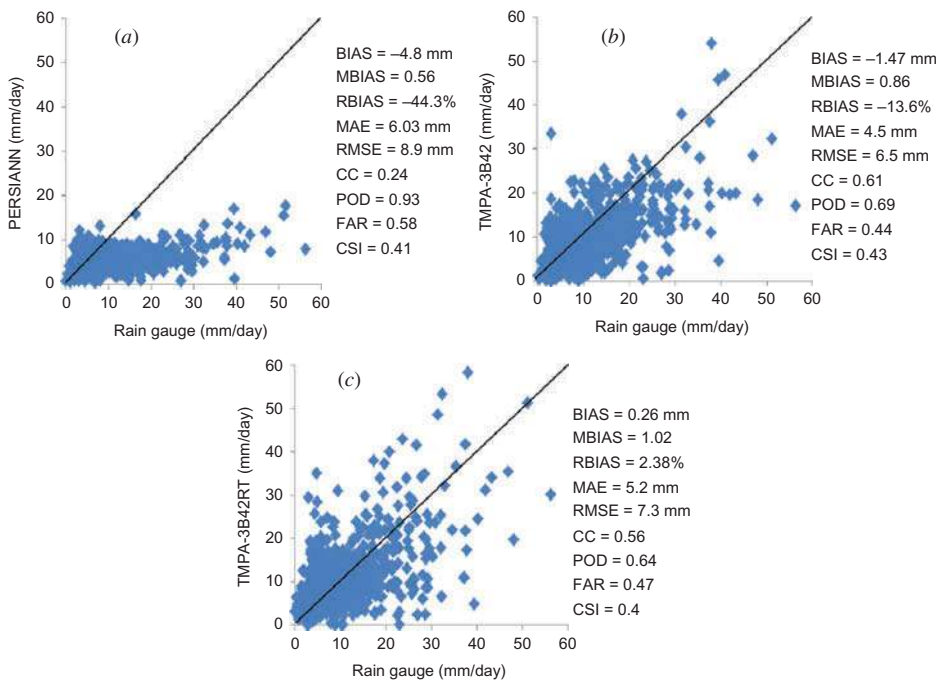


Figure 4. Scatter plots of daily averaged values for (a) PERSIANN, (b) 3B42V7, and (c) 3B42RT rainfall products versus rain gauge observations over 900 marked selected grid boxes.

With information on the daily precision and spatial variations of the three satellite precipitation products, Figure 5 shows the spatial pattern of daily averaged MBias over the selected grid boxes in the study area. As seen in Figure 5(a), PERSIANN shows underestimation ($MBias < 1$) for around 65% of the grid boxes in different regions including the central-western and southwestern parts of the country, particularly in the area of the Zagros Mountains. Furthermore, PERSIANN overestimated rainfall in some coastal regions close to the Caspian Sea and also in the northwestern and eastern regions of the country. The MBias value of PERSIANN ranges between 0.75 and 1.25 in some parts of the Alborz

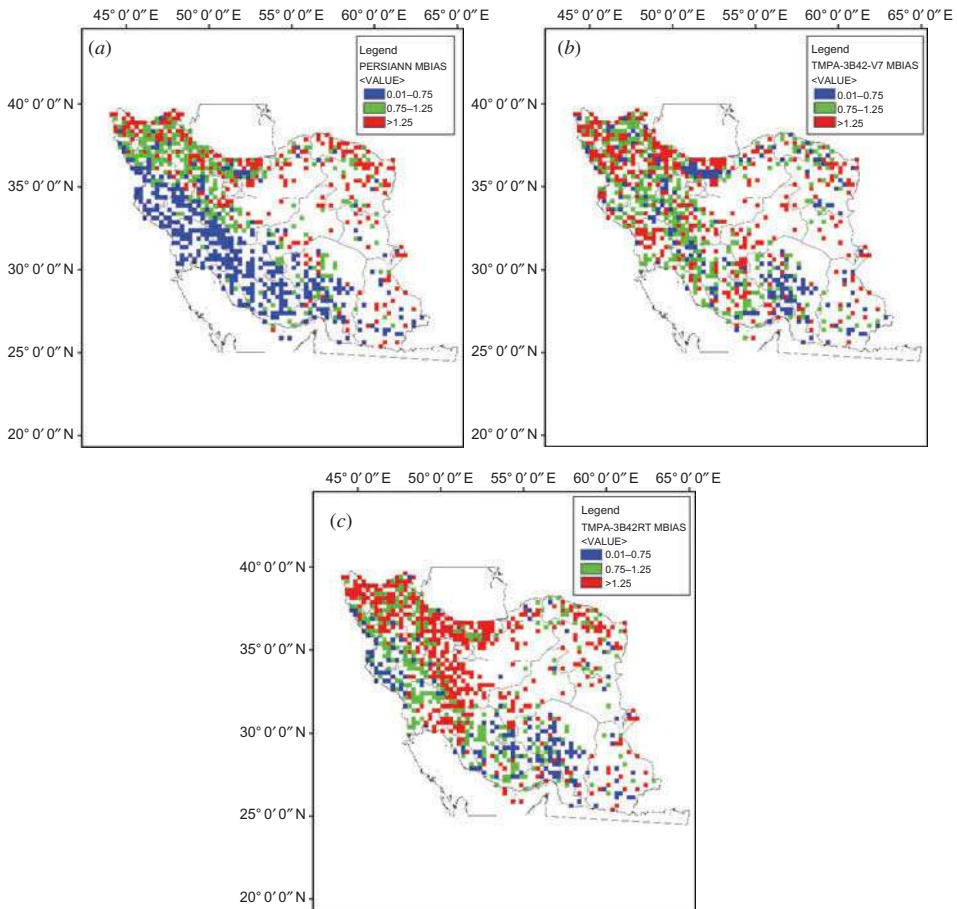


Figure 5. Spatial distribution of MBias for (a) PERSIANN, (b) 3B42V7, and (c) 3B42RT over the study area for average value of daily rainfall events at each grid box.

Mountains, Caspian Sea coastal areas, and northwest of the country. It is assumed that in MBias range 0.75–1.25, the satellite products have reasonable agreement with the gauge data. According to Figures 5(b) and (c), both products of TMPA show overestimation near the Caspian Sea and the northwest, but underestimation over the central-southern parts of the country. Also, 3B42V7 demonstrates reasonably accurate estimations (MBias 0.75–1.25) in most parts of the Zagros Mountains and in small parts of the northwest, while 3B42RT overestimated rainfall over those regions.

Figures 6(a) and (b) present the country-averaged values of POD and FAR for each selected event. Comparison of the three satellite products implies that PERSIANN data led to more accurate estimation of detecting precipitation, although its FAR is higher than that of 3B42V7 and 3B42RT. The spatial distribution of daily averaged values for POD and FAR over the entire country are shown in Figures 7 and 8. As seen in these figures, in regard to POD, both 3B42V7 and 3B42RT obtained better values in the western parts of country, particularly in the Zagros Mountains (Figures 7(b) and (c)). However, both products exhibit a poor value for POD in the eastern regions. In regard to FAR, Figure 8 indicates that all three satellite products gave more accurate estimation of FAR over the western regions and the Caspian Sea coastal areas than in the eastern regions of the country. Overall, the most

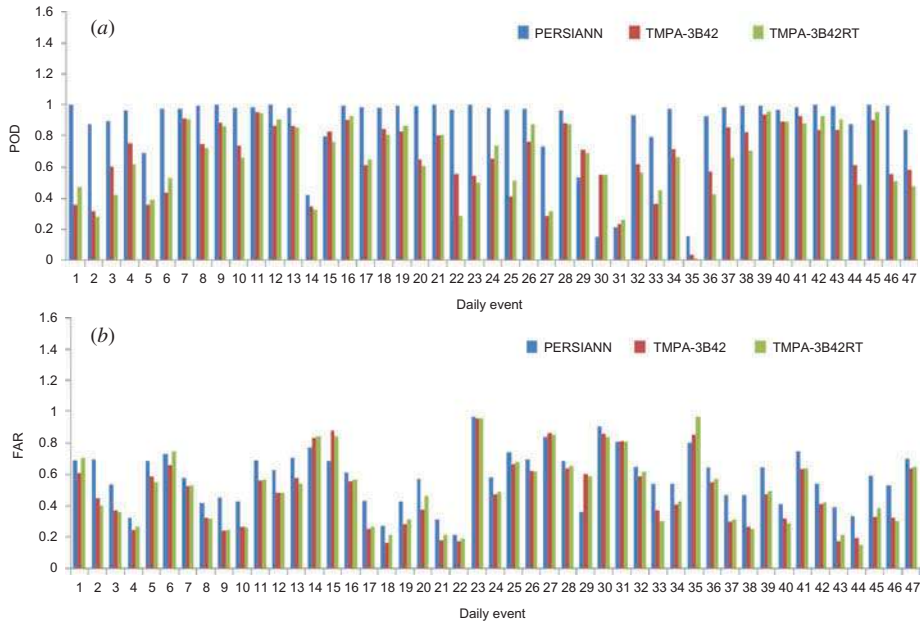


Figure 6. Daily values of (a) POD and (b) FAR for the three satellite products, spatially averaged over 900 selected grid boxes.

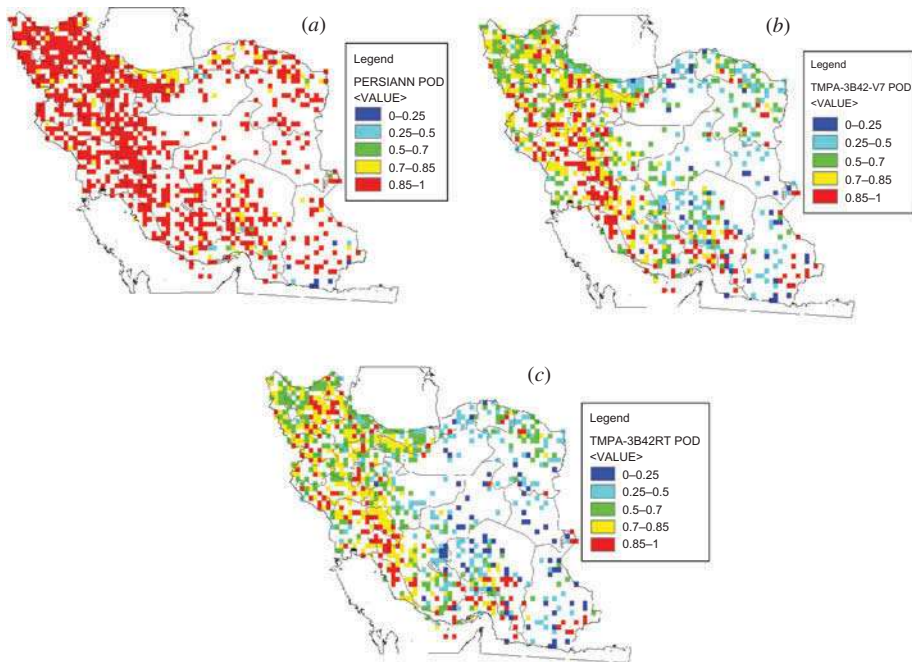


Figure 7. Spatial distribution of POD for (a) PERSIANN, (b) 3B42V7, and (c) 3B42RT over the study area for average value daily rainfall events at each grid box.

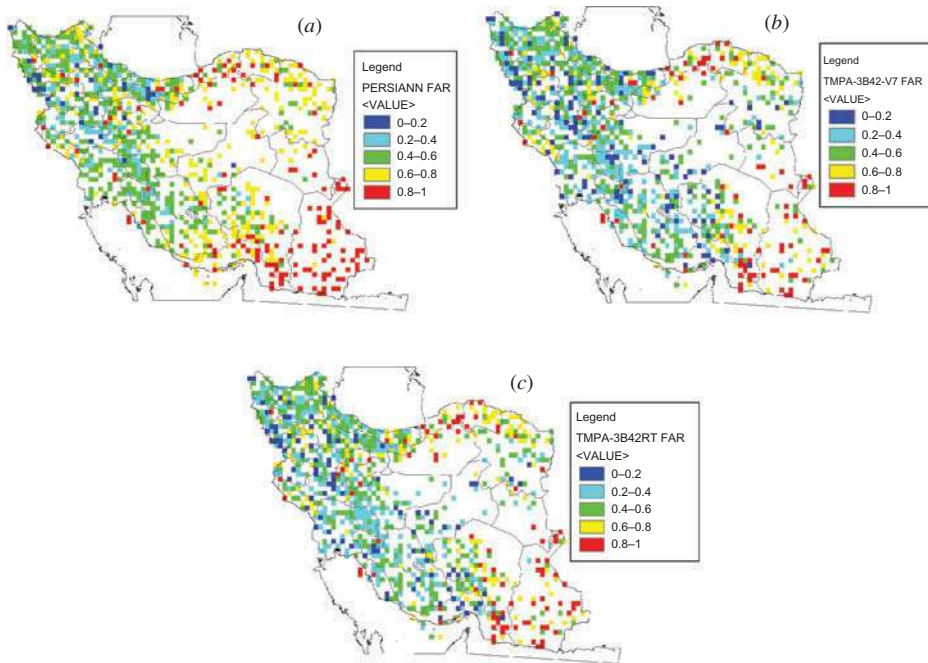


Figure 8. Spatial distribution of FAR for (a) PERSIANN, (b) 3B42V7, and (c) 3B42RT over the study area for average value of daily rainfall events at each grid box.

robust results for both POD and FAR for all three satellite products were obtained in the area of the Zagros Mountains.

The final key result of this study is shown in the graphs in Figure 9, which compare the daily averaged value of satellite precipitation products and rain gauge observations. As shown in Figures 9(a)–(c), the satellite data exhibit underestimation for rainfall thresholds higher than 10 mm/day. However, for PERSIANN, more grid boxes yielded underestimated values than did TMPA products. In general, the evaluation demonstrates that none of the satellite precipitation products can estimate moderate and heavy rainfall ($>10 \text{ mm d}^{-1}$) events reliably over Iran. The weakness of a single satellite precipitation product in detecting extreme events has been argued previously by AghaKouchak et al. (2011). It will be noted that the diamonds, triangles, and circles in Figures 9(a)–(c) represents an average value of daily rainfall events as estimated by PERSIANN, 3B42V7, and 3B42RT, respectively, over each selected grid box. The blue line in these figures denotes the average value of daily rainfall events as measured by rain gauges. For clarity, these values are ordered from lowest to highest.

5. Summary and conclusions

Reliable estimation and quantification of precipitation is essential for hydrological applications. However, in most parts of the world, particularly in developing countries like Iran, ground-based measurements provide poor spatial and temporal sampling of precipitation due to the absence of a dense network of rain gauge data. Furthermore, radar rainfall data are not available for most regions of Iran. Therefore, satellite-based rainfall estimates providing high spatial coverage of data over different terrains may be appropriate alternatives to rain gauges and radar measurements.

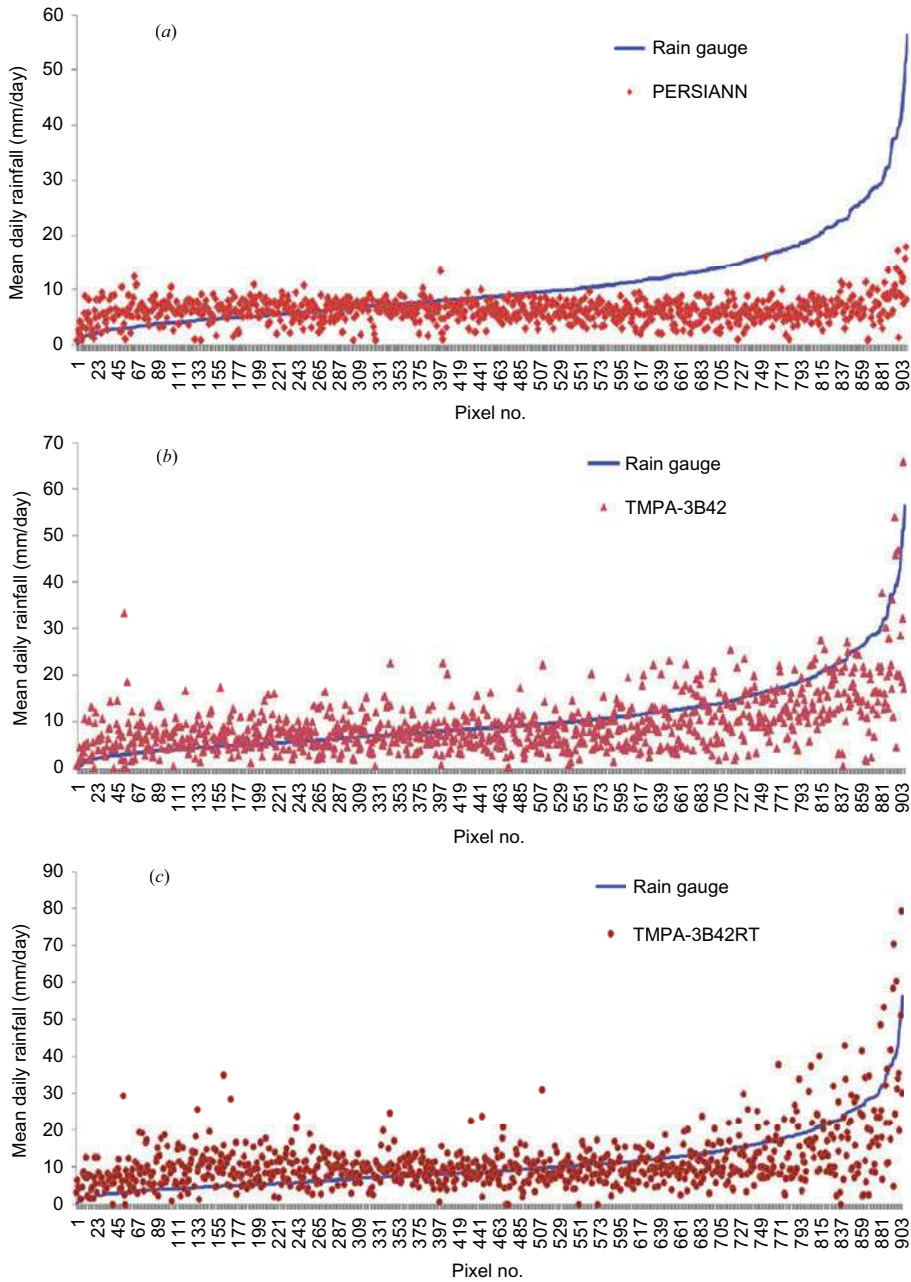


Figure 9. Comparison of daily rainfall averaged value at each grid box between gauge observations and (a) PERSIANN, (b) 3B42V7, and (c) 3B42RT data (rain gauge values are ordered from lowest to highest).

According to this study, one can generally conclude that microwave (MW)-based TMPA products perform better than infrared (IR)-based PERSIANN products over Iran. Also, because of the correction process against monthly gauge measurements, the bias-adjusted 3B42V7 product of TMPA shows a marked improvement over the real-time 3B42RT

product and has better correspondence with rain gauge observations compared with other satellite precipitation products. This finding is consistent with the results from studies by Sapiano and Arkin (2009), Sohn, Han, and Seo (2010), Romilly and Gebremichael (2011), and Gao and Liu (2013) over other regions.

The bias in the SREs depends on the rainfall patterns, and, in some cases, the elevation (Romilly and Gebremichael 2011). Overall, for the SREs studied here, the different values of bias ratio over the various regions can be interpreted as follows.

- (1) Along the central part of the Zagros Mountains with a highland topography, the local orographic effects may lead to positive and/or negative bias in SREs. Note that PERSIANN underestimates while 3B42RT overestimates rainfall over this region.
- (2) In the southwestern part close the Persian Gulf with a warm and tropical climate, the precipitation type is almost always convective. Across this area PERSIANN indicates underestimation, which is in agreement with the findings of Hong et al. (2007). Since PERSIANN is mainly based on IR brightness temperatures, the correlation between IR brightness temperature and rainfall is weak if little water is available in air profiles (Gao and Liu 2013). Also, Hong et al. (2007) argued that in light precipitation events, PERSIANN has difficulty estimating precipitation in comparatively shallow and warm (i.e. non-ice) convective clouds. However, both TMPA products gave reasonably accurate estimations over the southwestern part of country with convective rainfall.
- (3) Across the low- and mid-elevation areas in the western part of country with a temperate climate, the rainfall type is almost always stratiform. It should be noted that in this region, the stratiform precipitation is caused when warm air from Iraq (the western neighbour of Iran) meets cooler air from the Zagros Mountains. PERSIANN tends to underestimate over this area because of its IR-based algorithm. Huffman et al. (2010) concluded that stratiform clouds that tend to dominate in the cool season and frontal conditions lead to significant mis-estimation using IR algorithms. Nevertheless, in this region, 3B42RT showed low bias values of rainfall estimation consistent with results obtained by Ebert, Janowiak, and Kidd (2007).
- (4) PERSIANN shows a reasonable agreement in rain gauge observations over most parts of the northwestern area and some parts of the Alborz Mountains. There are heavy rainfall events across these regions, and thus the correlation between IR brightness temperature and rainfall is strong. Notice that these areas experience cold weather, so the overestimation by 3B42RT may be associated with an increase in ice aloft which is perceived by the MW sensors to be precipitation (Romilly and Gebremichael 2011).
- (5) In a semi-arid climate, raindrops may evaporate before reaching the surface (Tefragiorgis et al. 2011). Therefore, in the northeastern area of Iran covered by a semi-arid climate, both PERSIANN and 3B42RT led to overestimation.
- (6) Over the highland topography in the southeastern parts of country where PERSIANN underestimated rainfall, this may have been due to the poor detection of light rainfall events. Note that in this region because of the arid climate, precipitation is almost always light. Hong et al. (2007) explained that the bias of PERSIANN is dependent on elevation, which is characterized by an underestimation of the occurrence of light precipitation at high elevations and an overestimation of the occurrence of moderate-to-heavy precipitation at low elevations. Also, TMPA products showed underestimation in this area due to the local orographic effects.

- (7) In regard to accurate detection of rainfall events by SREs, all three products showed higher FAR across the eastern part of country, which is covered by an arid or semi-arid climate. As mentioned previously, the reason for this finding may be the evaporation of raindrops before reaching the surface in regions with an arid climate. However, in the western part with humid weather, all products studied showed better estimation of FAR. Furthermore, because of light precipitation across the eastern area, TMPA products demonstrated poor estimation of POD. Ebert, Janowiak, and Kidd (2007) inferred that MW-based TMPA tends to outperform models in warm/convective conditions, and vice versa in cool-season stratiform conditions. Therefore, across the western area with convective and stratiform precipitation, TMPA products yielded larger POD values. It is worthwhile to point out that since all three SREs showed poor values for FAR, the high values of POD should be interpreted along with the corresponding FARs.
- (8) In general, all three SREs tended to overestimate light rainfall ($0-10 \text{ mmd}^{-1}$) and underestimate moderate and heavy rainfall ($>10 \text{ mmd}^{-1}$).

The analysis presented in this study provides an overview of comparison between three SREs and daily rain gauge data in different parts of Iran. These satellite products were selected because they are available at similar spatial resolution, as well as being the most widely used over various regions around the world. Therefore, as a first attempt to evaluate different types of SREs over Iran, the authors focused on PERSIANN and TMPA products. However, in future research, other SREs (i.e. CMORPH, GSMaP) can be evaluated across this country. Moreover, training a satellite-retrieved precipitation algorithm on data from Iran may lead to more accurate estimations over this country.

Among the difficulties and limitations of this study were a shortage of continuous daily rain gauge data sets covering a reasonable period (i.e. 3 years or more), as well as limited and unevenly distributed rain gauges over the study area. Furthermore, due to the absence of a dense network of rain gauges, many of the selected grid boxes included only one rain gauge; to provide more accurate and reliable analyses of satellite precipitation estimates, particularly in the field of extreme events, grid boxes with more than two or three rain gauges are necessary.

It is emphasized that the conclusions derived from this study are based on available satellite-based and rain gauge data sets. The authors acknowledge that spatial and temporal uncertainties may exist when comparing different satellite products with ground-based observations. This work was intended to contribute to the ongoing research on uncertainty analysis of satellite precipitation products and bias-adjusted techniques to improve SREs.

Acknowledgements

The authors would like to thank the two anonymous reviewers whose comments helped to improve the presentation of this article significantly.

References

- AghaKouchak, A., A. Behrangi, S. Sorooshian, K. Hsu, and E. Amitai. 2011. "Evaluation of Satellite-Retrieved Extreme Precipitation Rates Across the Central United States." *Journal of Geophysical Research* 116: D02115. doi:10.1029/2010JD014741.
- AghaKouchak, A., A. Mehran, H. Norouzi, and A. Behrangi. 2012. "Systematic and Random Error Components in Satellite Precipitation Data Sets." *Geophysical Research Letters* 39: L09406. doi:10.1029/2012GL051592.

- As-Syakur, A. R., T. Tanaka, R. Prasetia, I. K. Swardika, and I. W. Kasa. 2010. "Comparison of TRMM Multisatellite Precipitation Analysis (TMPA) Products and Daily-Monthly Gauge Data over Bali Island." *International Journal of Remote Sensing* 32: 8969–8982. doi:10.1080/01431161.531784.
- Behrangi, A., B. Khakbaz, T. C. Jaw, A. AghaKouchak, K. Hsu, and S. Sorooshian. 2011. "Hydrologic Evaluation of Satellite Precipitation Products over a Mid-Size Basin." *Journal of Hydrology* 397: 225–237. doi:10.1016/j.jhydrol.11.043.
- Bitew, M. M., and M. Gebremichael. 2011. "Evaluation of Satellite Rainfall Products Through Hydrologic Simulation in a Fully Distributed Hydrologic Model." *Water Resources Research* 47: W06526. doi:10.1029/WR009917.
- Dinku, T., S. J. Connor, and P. Ceccato. 2010. "Comparison of CMORPH and TRMM-3B42 over Mountainous Regions of Africa and South America." In *Satellite Rainfall Applications for Surface Hydrology*, edited by M. Gebremichael and F. Hossain, 193–204. Dordrecht: Springer.
- Ebert, E. E., J. E. Janowiak, and C. Kidd. 2007. "Comparison of Near-Real-Time Precipitation Estimates from Satellite Observations and Numerical Models." *Bulletin of the American Meteorological Society* 88: 47–64. doi:10.1175/bams-88-1-47.
- Gao, Y. C., and M. F. Liu. 2013. "Evaluation of High-Resolution Satellite Precipitation Products Using Rain Gauge Observations over the Tibetan Plateau." *Hydrology and Earth System Sciences* 17: 837–849.
- Habib, E., A. Henschke, and R. Adler. 2009. "Evaluation of TMPA Satellite-Based Research and Real-Time Rainfall Estimates During Six Tropical-Related Heavy Rainfall Events over Louisiana, USA." *Atmospheric Research* 94: 373–388. doi:10.1016/j.atmosres.2009.06.015.
- Hirpa, F. A., M. Gebremichael, and T. Hopson. 2010. "Evaluation of High Resolution Satellite Precipitation Products over Very Complex Terrain in Ethiopia." *Journal of Applied Meteorology and Climatology* 49: 1044–1051. doi:10.1175/JAMC2298.1.
- Hong, Y., D. Gochis, J. Cheng, K. Hsu, and S. Sorooshian. 2007. "Evaluation of PERSIANN-CCS Rainfall Measurement Using the NAME Event Rain Gauge Network." *Journal of Hydrometeorology* 8: 469–482. doi:10.1175/JHM574.1.
- Hong, Y., K. Hsu, H. Moradkhani, and S. Sorooshian. 2006. "Uncertainty Quantification of Satellite Precipitation Estimation and Monte Carlo Assessment of the Error Propagation into Hydrologic Response." *Water Resources Research* 42: W08421. doi:10.1029/WR004398.
- Hong, Y., K. L. Hsu, S. Sorooshian, and X. G. Gao. 2004. "Precipitation Estimation from Remotely Sensed Imagery Using an Artificial Neural Network Cloud Classification System." *Journal of Applied Meteorology* 43: 1834–1852.
- Hsu, K. L., X. Gao, S. Sorooshian, and H. V. Gupta. 1997. "Precipitation Estimation from Remotely Sensed Information Using Artificial Neural Networks." *Journal of Applied Meteorology* 36: 1176–1190.
- Huffman, G. J., R. Adler, D. Bolvin, G. Gu, E. Nelkin, K. Bowman, E. Stocker, and D. Wolff. 2007. "The TRMM Multi-Satellite Precipitation Analysis: Quasiglobal, Multi-Year, Combined-Sensor Precipitation Estimates at Fine Scale." *Journal of Hydrometeorology* 8: 38–55.
- Huffman, G. J., R. F. Adler, D. T. Bolvin, and E. J. Nelkin. 2010. "The TRMM Multisatellite Precipitation Analysis (TMPA)." In *Satellite Applications for Surface Hydrology*, edited by M. Gebremichael and F. Hossain, 3–22. Dordrecht: Springer.
- Huffman, G. J., and D. T. Bolvin. 2012. "TRMM and Other Data Precipitation Data Set Documentation." Laboratory for Atmospheres, NASA Goddard Space Flight Center and Science Systems and Applications.
- Huffman, G. J., D. T. Bolvin, E. J. Nelkin, and R. F. Adler. 2011. "Highlights of Version 7 TRMM Multi-Satellite Precipitation Analysis (TMPA)." In *5th International Precipitation Working Group Workshop, Workshop Program and Proceedings*, 11–15 October 2010, Hamburg, Germany, edited by C. Klepp and G. Huffman. Reports on Earth System Science, 100/2011, Max-Planck-Institut für Meteorologie. ISSN 1614–1199, 109–110.
- Hughes, D. A. 2006. "Comparison of Satellite Rainfall Data with Observations from Gauging Station Networks." *Journal of Hydrology* 327: 399–410.
- Javanmard, S., A. Yatagai, M. M. Nodzu, J. BodaghJamali, and H. Kawamoto. 2010. "Comparing High-Resolution Gridded Precipitation Data with Satellite Rainfall Estimate of TRMM_3B42 over Iran." *Advanced Geosciences* 25: 119–125.
- Jiang, S., L. Ren, Y. Hong, B. Yong, X. Yang, F. Yuan, and M. Ma. 2012. "Comprehensive Evaluation of Multi-Satellite Precipitation Products with a Dense Rain Gauge Network and Optimally

- Merging Their Simulated Hydrological Flows Using the Bayesian Model Averaging Method.” *Journal of Hydrology* 452–453: 213–225.
- Joyce, R. J., J. E. Janowiak, P. A. Arkin, and P. Xie. 2004. “CMORPH: A Method that Produces Global Precipitation Estimates from Passive Microwave and Infrared Data at High Spatial and Temporal Resolutions.” *Journal of Hydrometeorology* 5: 487–503.
- Kubota, T., T. Ushio, S. Shige, M. Kachi, and K. Okamoto. 2009. “Verification of High Resolution SREs Around Japan Using a Gauge-Calibrated Ground-Radar Dataset.” *Journal of the Meteorological Society of Japan* 87A: 203–222.
- Li, L., Y. Hong, J. Wang, R. F. Adler, F. S. Policelli, S. Habib, D. Irwn, T. Korme, and L. Okello. 2009. “Evaluation of the Real-Time TRMM-based Multi-Satellite Precipitation Analysis for an Operational Flood Prediction System in Nzoia Basin, Lake Victoria, Africa.” *Natural Hazards* 50: 109–123. doi:10.1007/s11069-0089324–5.
- Romilly, T. G., and M. Gebremichael. 2011. “Evaluation of Satellite Rainfall Estimates Over Ethiopian River Basins.” *Hydrology and Earth System Sciences* 15: 1505–1514.
- Sapiano, M. R. P., and P. A. Arkin. 2009. “An Intercomparison and Validation of High-Resolution Satellite Precipitation Estimates with 3-Hourly Gauge Data.” *Journal of Hydrometeorology* 10: 149–166. doi:10.1175/2008jhm1052.1.
- Sohn, B. J., H.-J. Han, and E.-K. Seo. 2010. “Validation of Satellite-Based High-Resolution Rainfall Products over the Korean Peninsula Using Data from a Dense Rain Gauge Network.” *Journal of Applied Meteorology and Climatology* 49: 701–714. doi:10.1175/2009jamc2266.1.
- Sorooshian, S., K. Hsu, X. Gao, H. V. Gupta, B. Imam, and D. Braithwaite. 2000. “Evolution of the PERSIANN System Satellite-Based Estimates of Tropical Rainfall.” *Bulletin of the American Meteorological Society* 81: 2035–2046.
- Su, F., Y. Hong, and D. P. Lettenmaier. 2008. “Evaluation of TRMM Multisatellite Precipitation Analysis (TMPA) and Its Utility in Hydrologic Prediction in the La Plata Basin.” *Journal of Hydrometeorology* 9: 622–640. doi:10.1175/JHM944.1.
- Tesfagiorgis, K., S. E. Mahani, N. Y. Krakauer, and R. Khanbilvardi. 2011. “Bias Correction of Satellite Rainfall Estimates Using a Radar-Gauge Product – A Case Study in Oklahoma (USA).” *Hydrology and Earth System Sciences* 15: 2631–2647.
- Tian, Y., C. D. Lidard-Peters, B. J. Choudhury, and M. Garcia. 2007. “Multitemporal Analysis of TRMM-Based Satellite Precipitation Products for Land Data Assimilation Applications.” *Journal of Hydrometeorology* 8: 1165–1183. doi:10.1175/2007JHM859.1.
- Turk, F. J., and S. D. Miller. 2005. “Toward Improving Estimates of Remotely-Sensed Precipitation with MODIS/AMSR-E Blended Data Techniques.” *IEEE Transactions on Geoscience and Remote Sensing* 43: 1059–1069.
- Ushio, T., K. Sasashige, T. Kubota, S. Shige, K. Okamoto, K. Aonashi, N. Inoue, T. Takahashi, M. Iguchi, R. Kachi, and T. Oki. 2009. “A Kalman Filter Approach to the Global Satellite Mapping of Precipitation (GSMaP) from Combined Passive Microwave and Infrared Radiometric Data.” *Journal of the Meteorological Society of Japan* 87A: 137–151.
- Wilks, D. S. 2006. *Statistical Methods in the Atmospheric Sciences*. 2nd ed., 627 pp. Burlington, MA: Academic Press.
- Xie, P., A. Yatagai, M. Chen, T. Hayasaka, Y. Fukushima, L. Changming, and S. Yang. 2007. “A Gauge-Based Analysis of Daily Precipitation Over East Asia.” *Journal of Hydrometeorology* 8: 607–626.
- Yatagai, A., P. Xie, and P. Alpert. 2008. “Development of a Daily Gridded Precipitation Data for the Middle East.” *Advances in Geosciences* 12: 165–170.
- Yong, B., Y. Hong, L. L. Ren, J. J. Gourley, G. J. Huffman, X. Chen, W. Wang, and I. S. Khan. 2012. “Assessment of Evolving TRMM-Based Multisatellite Real-Time Precipitation Estimation Methods and Their Impacts on Hydrologic Prediction in a High Latitude Basin.” *Journal of Geophysical Research* 117: D09108. doi:10.1029/2011JD017069.
- Yong, B., L. L. Ren, Y. Hong, J. H. Wang, J. J. Gourley, S. H. Jiang, X. Chen, and W. Wang. 2010. “Hydrologic Evaluation of Multisatellite Precipitation Analysis Standard Precipitation Products in Basins Beyond Its Inclined Latitude Band: A Case Study in Laohahe Basin, China.” *Water Resources Research* 46: W07542. doi:10.1029/WR008965.